Journal of Cellular Biochemistry 93:120–132 (2004)

Post-Transcriptional Control of Expression of sFlt-1, an Endogenous Inhibitor of Vascular Endothelial Growth Factor

William R. Huckle* and Rebecca I. Roche

Department of Biomedical Sciences and Pathobiology, Virginia-Maryland Regional College of Veterinary Medicine, Virginia Tech, Blacksburg, Virginia 24061

Abstract Vascular endothelial growth factor (VEGF) is a major modulator of angiogenesis. Biological effects of VEGF are mediated by endothelial cell-surface receptors, KDR and Flt-1. Alternative Flt-1 RNA processing, involving retention of intron 13 and the use of intronic cleavage-polyadenylation signals, produces a secreted form of Flt-1, ''sFlt-1,'' that binds VEGF with high affinity and can inhibit VEGF signaling. To probe mechanisms controlling sFlt-1 expression, we have cloned and sequenced Flt-1 intron 13 from a mouse genomic library and located RNA processing signals potentially involved in sFlt-1 mRNA formation. A minigene construct containing Flt-1 intron 13 directed the expression of both secreted (i.e., cleaved/polyadenylated) and transmembrane (i.e., spliced) forms of Flt-1 mRNA and protein. Using rapid amplification of 3′ cDNA ends (3′-RACE) and quantitative PCR (QPCR) analysis to test the activity of intronic cleavage-polyadenylation signals, we observed that multiple sites were utilized for sFlt-1 mRNA processing in both native tissues and Flt-1 minigene transfectants. In transfectants, the most distal signal was utilized preferentially. The potential for interaction between pathways leading to sFlt-1 or full-length Flt-1 was evaluated using QPCR to measure relevant mRNAs after transfection with signal mutants. Decreased expression of sFlt-1 mRNA in cleavage-polyadenylation mutants was accompanied by reciprocal increases in full-length Flt-1 mRNA. Multiple sFlt-1 mRNA species are formed that differ by up to 3.9 kb in their 3′-untranslated regions (UTRs), which contain sites of potential regulatory importance. The reciprocity between sFlt-1 and Flt-1 mRNA expression suggests a novel post-transcriptional mechanism by which sFlt-1 protein production and, thereby, responsiveness to VEGF, may be modulated. J. Cell. Biochem. 93: 120–132, 2004.

Key words: vascular endothelial growth factor; Flt-1; RNA processing; receptor

The formation of new blood vessels, or angiogenesis, is a vital, dynamic process in vertebrate organisms. Well-regulated angiogenesis is essential for normal tissue growth, wound healing, cyclical endometrial hyperplasia, and pregnancy [Nguyen and D'Amore, 2001]. Moreover, angiogenesis can be a beneficial adaptation to myocardial ischemia or peripheral vascular insufficiency [Carmeliet, 2003]. Recent research has identified a variety of endothelial-selective mitogens, chemotactic agents, and differentiation factors, such as vascular endothelial growth factor (VEGF) and the angiopoietins [Yancopoulos et al., 2000; Gerber and Ferrara, 2003] that act in concert to promote the formation or maintenance of functional vasculature. Overexpression of VEGF has been linked with a variety of vascular pathologies, including tumor angiogenesis [Folkman, 2001; Los and Voest, 2001], diabetic retinopathy [Spranger and Pfeiffer, 2001], and atherosclerotic plaque progression [Celletti et al., 2001]. A variety of clinical approaches to inhibiting VEGF-driven neovascularization are being evaluated [Kim et al., 1993; Shawver et al., 1997; Prewett et al., 1999; Pavco et al., 2000]. At the same time, VEGF and related angiogenic growth factors are likely contributors to adaptive angiogenesis occurring in ischemic muscle

Grant sponsor: American Cancer Society Institutional Research; Grant number: #IRG-99-225-01; Grant sponsor: American Heart Association Mid-Atlantic Affiliate; Grant number: #0256377U.

*Correspondence to: Dr. William R. Huckle, College of Veterinary Medicine, Phase II, Duckpond Drive (0442), Virginia Tech, Blacksburg, VA 24061.
E-mail: wrhuckle@vt.edu

Received 8 January 2004; Accepted 11 March 2004
DOI 10.1002/jcb.20142
Published online 17 June 2004 in Wiley InterScience (www.interscience.wiley.com).

and have potential as pro-angiogenic therapeutics [Epstein et al., 2001].

Angiogenic responses to VEGF are mediated by two cell-surface receptors, Flt-1 and KDR, whose expression is largely restricted to endothelial cells [Shibuya et al., 1990; Finnerty et al., 1993; Choi et al., 1994; Yamane et al., 1994]. Alternative processing of Flt-1 pre-mRNA, involving retention of intron 13 [Kondo et al., 1998], produces a secreted form of Flt-1 ("sFlt-1"; Fig. 1A) that binds VEGF with high affinity ($K_d \sim 20$ pM) [Kendall and Thomas, 1993]. In vivo, overexpression of sFlt-1, either in stably transfected cells [Goldman et al., 1998; Siemeister et al., 1999] or after administration of adenoviral vectors [Kong et al., 1998; Shiose et al., 2000; Takayama et al., 2000], can dramatically inhibit growth of tumor xenografts in mice. Although it is clear that exogenous sFlt-1 can dramatically inhibit biological actions of VEGF, little is known about the normal function(s) of sFlt-1 or the mechanisms controlling its biosynthesis. Available evidence suggests that the relative abundance of mRNAs for sFlt-1 and full-length Flt-1 can vary physiologically [Clark et al., 1998; He et al., 1999; Krussel et al., 1999], suggesting that regulated expression of sFlt-1 is an important determinant of responsiveness to VEGF in embryonic development, adult vascular homeostasis, and angiogenic pathologies [Graubert et al., 2001]. In the present work, we define RNA sites involved in sFlt-1

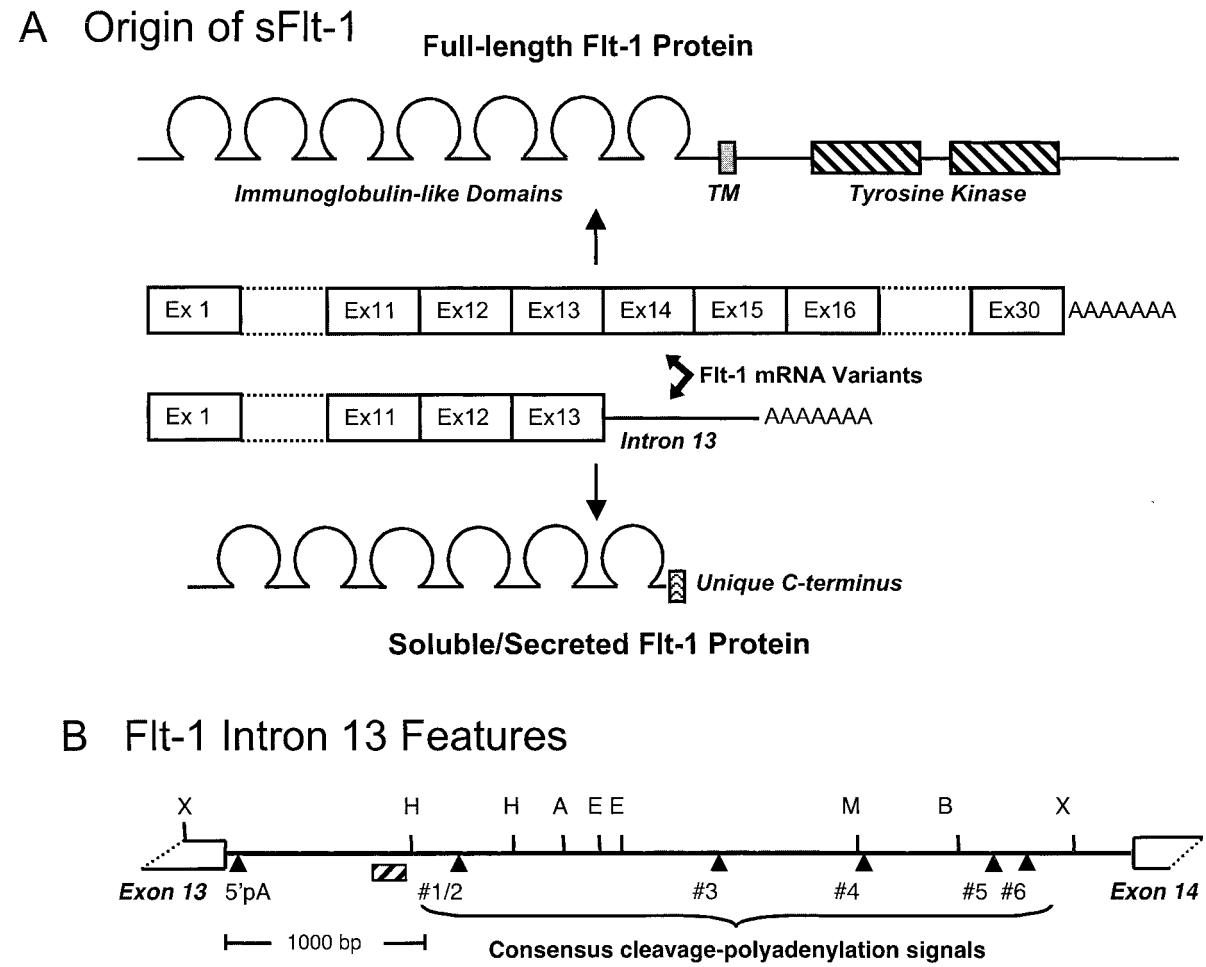

Fig. 1. Flt-1 protein, mRNA, and genomic structures. **A**: Alternative pre-mRNA processing gives rise to membrane-anchored and secreted forms of Flt-1. sFlt-1 protein retains the first six immunoglobulin-like domains of Flt-1, including the domains that contain the major VEGF-binding determinants [Barleon et al., 1997]. The transmembrane (TM) and intracellular regions, encoded by exons 16–30, are excluded from sFlt-1, which instead contains a unique 31-amino acid C-terminal peptide encoded by the 5′-end of intron 13. **B**: Scale map of Flt-1 intron 13 indicating sites of consensus cleavage-polyadenylation signals #1–6, the 5′-polyadenylation site ("5′-pA") previously reported [He et al., 1999], and restriction endonuclease cleavage by *Xba*I (X), *Hind*III (H), *Age*I (A), *Mlu*I (M), and *Btr*I (B). Striped bar, hybridization probe for genomic library screening.

mRNA formation and test interactions between pathways that generate sFlt-1 or full-length Flt-1 mRNA from a common pre-mRNA transcript. A preliminary account of a portion of this work has appeared previously in abstract form [Huckle and Roche, 2001].

MATERIALS AND METHODS

Flt-1 Intron 13 Cloning and Sequencing

A genomic BAC library from C57BL/6J mice (RPCI-23 [Osoegawa et al., 2000]; Research Genetics) was screened by hybridization with a 174-bp probe corresponding to sequence near the 3′-untranslated region (UTR) of mouse sFlt-1 cDNA [Kondo et al., 1998] (Fig. 1B). The probe was prepared by PCR amplification using 0.25 μM primers 226 and 227 (Table I), 1× Taq PCR Mastermix (Qiagen), and cDNA template from mouse lung (20-μl reaction; 30 cycles; 94°C denaturation/1 min, 55.7°C annealing/1 min, 72°C elongation/2 min). A selected positive BAC plasmid was purified (Clontech NucleoBond BAC Maxi-columns) and digested with *Eco*RI or *Hind*III (New England Biolabs). Gel-fractionated DNA fragments were purified (Qiaex II, Qiagen) and ligated into pLITMUS38. DH5α transformants were screened by PCR for the presence of either the exon 13-intron 13 junction (primers 205/204) or exon 14 (220/206). Four subclones encompassing all of intron 13 were isolated for plasmid purification (Qiagen Midiprep) and DNA sequencing by dye termination (PE Biosystems). Contiguous sequence data were assembled using the SeqMan module of the DNAStar sequence analysis suite.

Quantitative PCR (QPCR) Analysis

Fluorogenic TaqMan® probes [Livak et al., 1995] and PCR primers were designed using Primer Express software (PE Biosystems) to detect cDNAs containing the exon 13-exon 14 junction (Flt-1), the exon 13-intron 13 junction ("total sFlt-1"), the intronic region between cleavage-polyadenylation signals #4 and #5 ("long sFlt-1"), and neo^R derived from pcDNA3

TABLE I. Primer and Probe Sequences

Name	Location/use	Sequence (5′ → 3′)
201	Exon 1 (ss)	GGCTGCAGGCGCGGAGAAGG
202	Exon 10 (as)	GGTGACAGGGGTGCCAGAGC
203	Exon 9 (ss)	AACCGAGGATGCAGGGGACTAT
204	Intron 13 (as)	AGGGCACTGGGCTTTCTTATTAC
205	Exon 13 (ss)	AGAAGACTCGGGCACCTATG
206	Exon 14 (as)	GGCGCGGGGACACCTCTA
209	Exon 3 (ss)	CTGCAGCACCTTGACCTTGGACAC
216	Exon 13 (ss)	AAGATGCCAGCCGAAGGAGAGGAC
217	Exon 30 (as)	CTTTAGGCGGGCGGGGAGGAGTA
220	Exon 14 (ss)	GGTCTCCATCAGTGGCTCTACGACCTT
226	Intron 13 (ss)	GAATTATGAAGGTCCAGCAGGTCT
227	Intron 13 (as)	CCCAGGGGCCATGAGTGTTTA
238	Intron 13 (ss)	CTCTGGATTTCTGCCCTAGGATTTGC
242	Intron 13 (ss)	AACCAGCACTTCCTTCAACGCGTG
244	Intron 13 (ss)	AGTTGTCTGGGCACTGTTGAATGCT
278	Intron 13 (ss)	CTTGTGGGTGGCTGTCTTTAGCTACTCA
211	QPCR total sFlt-1 (ss)	GGGAAGACATCCTTCGGAAGA
212	QPCR total sFlt-1 (as)	TCCGAGAGAAAATGGCCTTTT
TP1	QPCR probe, total sFlt-1	6FAM-CCGCAGTGCTCACCTCTAACGAGAACTTCT-TAMRA
228	QPCR Flt-1 (ss)	TTCGGAAGACAGAAGTTCTCGTT
229	QPCR Flt-1 (as)	GACCTCGTAGTCACTGAGGTTTTG
TP3	QPCR probe, Flt-1	6FAM-AGATTCGGAAGCGCCACACCTGCT-TAMRA
296	QPCR neo^R (ss)	GCGCCCGGTTCTTTTTGT
297	QPCR neo^R (as)	GCCTCGTCCTGCAGTTCATT
TP5	QPCR probe, neo^R	6FAM-AAGACCGACCTGTCCGGTGCCCT-TAMRA
312	QPCR long sFlt-1 (ss)	AAGGGTGCAGAATATGTAAGGGATA
313	QPCR long sFlt-1 (as)	GCCTTTCCCCCATCTCATTT
TP7	QPCR probe, long sFlt-1	6FAM-CAAGACCCTCTGGATTTCTGCCCTAGGATTT-TAMRA
268	Mut pA 5 (ss)	TGGCATTTTATTAA[CAGACA]TTGTATTGTA
269	Mut pA 5 (as)	TACAATACAATGTCTGTTAATAAAATGCCA
270	Mut pA 6 (ss)	GGAGGGGAGTGACC[GACAGA]GCATTGAAT
271	Mut pA 6 (as)	ATTCAATGCTCTGTCGGTCACTCCCCTCC
306	Mut NC (ss)	AGT[CAGACACAGTGCC]ATACTTGTGCTATT
307	Mut NC (as)	TGGCACTGTGTCTGACTTTCTCTTAAAACA

Sequences of primers and probes used for conventional PCR amplification, 3′-RACE analysis, and real-time PCR. ss, sense strand; as, antisense strand; QPCR, quantitative PCR; Mut pA, point mutation of polyadenylation signal; NC, non-canonical cleavage-polyadenylation signal; RT, reverse transcription. Boundaries of point-mutation sites are boxed.

(Table I). The specificity of these reagents was verified using purified plasmid templates. Equivalence of amplification efficiency [Livak and Schmittgen, 2001] for all targets was confirmed using dilutions of cDNAs prepared from mouse tissue (Ambion) or HEK293 transfectant RNAs. Triplicate 25-μl reactions contained TaqMan® Universal Master Mix (PE Biosystems), 0.3 μM primers, 0.2 μM probe, and random-primed cDNAs derived by reverse-transcription (SuperScript II; Life Technologies). Reactions were denatured at 95°C for 10 min, then cycled 40 times between 95°C (15 s) and 60°C (1 min) in a PE7700 Sequence Detection System. Negative control reactions contained either no template or equivalent quantities of RNA without prior reverse-transcription. Target gene expression levels were determined by the comparative threshold cycle (ΔΔCt) method [Livak et al., 2001]. In samples derived from transfected HEK293 cells, sFlt-1 or Flt-1 expression was first normalized to neo^R expression within each sample (ΔCt), then compared to neo^R-normalized sFlt-1 or Flt-1 level in wild-type pFIN13 transfectants (ΔΔCt). Data were subjected to ANOVA (Mixed-effects procedure, SAS) using unexponentiated ΔΔCt values derived from three to four independent experiments. For mouse tissue cDNA templates, comparisons of Flt-1:total sFlt-1 and long sFlt-1:total sFlt-1 mRNAs (ΔCt) were expressed relative to those in lung (ΔΔCt). mRNA ratios are given by $2^{-\Delta\Delta Ct}$.

Flt-1 and sFlt-1 Expression Constructs

Flt-1 and sFlt-1 coding sequences were obtained by PCR amplification of mouse lung cDNA using primers (Table I) designed to generate overlapping, 1,000–2,000-bp segments. Replicate, Pfu-blunted PCR products were subcloned into pPCR-Script (Stratagene) and sequenced to identify clones with the expected structure [Finnerty et al., 1993; Yamane et al., 1994]. sFlt-1 and full-length Flt-1 cDNAs were assembled into a pcDNA3-based vector for constitutive expression under the human cytomegalovirus (CMV) immediate-early promoter containing CMV intron A, yielding psFlt-1 and pFlt-1, respectively. To confirm expression of sFlt-1 and Flt-1 proteins, 3 μg of each vector was transfected into HEK293 cells (ATCC; 600,000 cells/60 mm dish) using 9-μl TransIT293 reagent (Mirus). We chose HEK293 cells as a host for expression studies because of their relative ease of transfection and the ability of QPCR to selectively measure expression of mouse Flt-1 and sFlt-1 mRNAs against the human sequence background. Conditioned media from transient or G418-selected stable transfectants were collected after 48 h, and sFlt-1 was isolated by adsorption to heparin-agarose beads (Sigma; 80 μl packed beads/5 ml medium) as described [Kendall et al., 1996]. Heparin beads were centrifuged, washed three times with 1-ml Dulbecco's phosphate buffered saline without Ca^{2+} and Mg^{2+} (DPBS), and adsorbed proteins were eluted by addition of 80-μl 2× SDS–PAGE Laemmli sample buffer (Sigma). Protein samples (25 μl) were separated on 8–16% gradient SDS–polyacrylamide minigels (BioWhittaker), transferred to Immobilon-P membranes (Millipore), and immunoblotted using antibodies reactive with either the Flt-1/sFlt-1 N-terminus or Flt-1 C-terminus (1:1,000; Santa Cruz), followed by chemiluminescent detection (SuperSignal, Pierce) and exposure to BioMax film (Kodak).

Flt-1 Minigene Constructs

A minigene construct (pFIN13), in which intron 13 was inserted between the cDNA sequences, derived from exons 1–13 and 14–30, was assembled by a 3-way ligation involving compatible fragments from psFlt-1, pFlt-1, and appropriate genomic subclones. Restriction endonuclease mapping and DNA sequencing confirmed integrity of the construct. Deletion mutants of pFIN13 were prepared by complete or partial restriction endonuclease digestion, blunt-ending when appropriate with Klenow fragment of DNA polymerase, religation, and transformation into DH5α. Point mutants of cleavage-polyadenylation signals were prepared using a two-stage, PCR-based approach [Ishii et al., 1998] and a pFIN13-derived cassette described elsewhere (Roche RI and Huckle WR, unpublished data).

Rapid Amplification of 3′ cDNA Ends (3′-RACE)

Two days after transfection with pFIN13 or null expression vector, HEK293 cells were washed with 5-ml DPBS and lysed for isolation of total RNA (Qiagen RNeasy with on-column DNase treatment). RNAs (2 μg) from transfectants or mouse lung (Ambion) were primed for reverse transcription using 3′-RACE adapter primer [Frohman et al., 1988]; first-strand cDNAs produced then were used as templates

for PCR amplification with Flt-1-specific primers plus an abridged universal adapter primer (AUAP). For mouse lung cDNA, a second, nested round of PCR was performed using 5% of the first-round product. PCR products were separated on 1% agarose gels, and selected bands (those appearing in material derived from pFIN13 but not null vector transfectants) were purified for A/U-dependent subcloning into pDrive (Qiagen). Recombinant inserts were sequenced to determine sites of sFlt-1 mRNA cleavage and polyadenylation.

RESULTS

Preliminary to probing the RNA processing mechanisms that control sFlt-1 and Flt-1 expression, we isolated and sequenced genomic clones that encompass mouse Flt-1 intron 13 and its flanking exons. Our intron 13 sequence (4701 bp; submitted as GenBank AF473823) was 99.38% identical to sequence reported for the Flt-1 gene on mouse chromosome 5 (NT_039324); strong agreement (99.4% sequence identity over 1171 bases) also was seen between our sequence and the intron 13-derived portions of sFlt-1 cDNA sequence reported previously [Kondo et al., 1998].

We scanned the intron 13 sequence to locate consensus recognition sites for nuclear cleavage-polyadenylation or splicing factors [Reed and Palandjian, 1997; Zhao et al., 1999]. Six occurrences of the canonical cleavage-polyadenylation signal AAUAAA were found in intron 13 (Fig. 1B), as well as six occurrences of the signal variant AUUAAA. The most proximal AUUAAA site likely signals cleavage-polyadenylation of an sFlt-1 mRNA 3′-end identified previously [He et al., 1999]. The first two canonical cleavage-polyadenylation signals, occurring as a tandem AAUAAA/AAUAAA sequence, were located approximately 40 nucleotides downstream of an internal A_{13} tract, identified as a presumed polyadenylation site by previous investigators [Kondo et al., 1998]. The other four occurrences of AAUAAA were spread across nearly the full length of the intron. Other consensus sites identified include the 5′- and 3′-splice sites, a candidate branchpoint sequence, and polypyrimidine tract, all characteristic of U2-dependent introns [Reed and Palandjian, 1997].

The finding of multiple putative cleavage-polyadenylation signals in Flt-1 intron 13 raises the possibility that sFlt-1 mRNAs distinct from that previously identified [He et al., 1999] may be formed. To ascertain whether the sFlt-1 mRNA pool normally contains species polyadenylated downstream of the most distal cleavage-polyadenylation signal, QPCR analysis was performed on cDNAs derived from a panel of mouse tissues (Fig. 2). These experiments confirmed that "long" sFlt-1 mRNAs are detectable, and further revealed that ratios of long sFlt-1:total sFlt-1 mRNAs can vary by up to 3.3-fold in different tissues. A similar range of tissue-to-tissue variation (3.5-fold) was noted in ratios of full-length Flt-1:total sFlt-1, consistent with the idea that physiological mechanisms exist to control relative expression of Flt-1 and sFlt-1 mRNAs.

To study Flt-1 RNA processing in a defined system, we prepared a minigene expression construct, "pFIN13," composed of Flt-1 exons 1–13, intron 13, and exons 14–30. To determine the location of the 3′-end(s) of sFlt-1 mRNAs transcribed from pFIN13, we transfected this construct or a null vector into HEK293 cells and analyzed total RNA pools by 3′-RACE. To amplify the previously reported transcript that is cleaved and polyadenylated just downstream

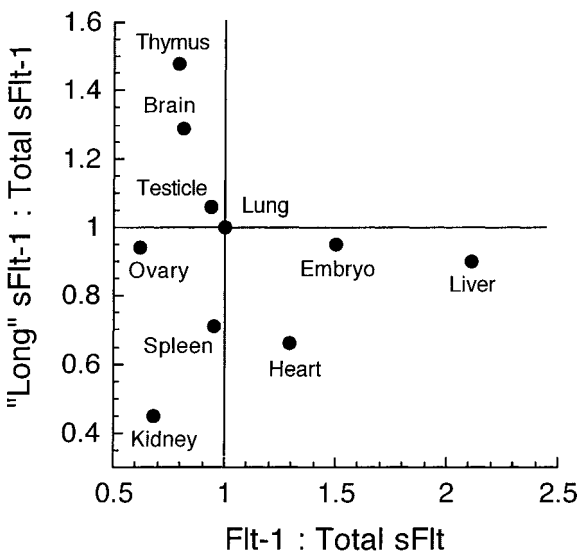

Fig. 2. Relative sFlt-1 and Flt-1 expression in mouse tissues. QPCR analysis was performed using primers and probes specific for cDNA derived from full-length Flt-1 mRNA (targeting spliced exon 13/14 junction), total sFlt-1 (exon 13/intron 13 junction), and long sFlt-1 (between cleavage-polyadenylation signals 4 and 5). For each set of comparisons, ΔΔCt values were determined by indexing ΔCt results for each tissue to that derived from lung; mRNA ratios then were calculated as $2^{-\Delta\Delta Ct}$ [Livak and Schmittgen, 2001].

of the predicted sFlt-1 translation stop [He et al., 1999], we used primer 209 that anneals in exon 3. As expected, sequencing of the 1,843-bp product isolated from 209/AUAP-amplified material revealed a cleavage-polyadenylation site identical to that reported by He et al. [1999] (Fig. 1B).

To capture novel cDNAs derived from transcripts terminating downstream of putative cleavage-polyadenylation signals #1–6, we used intron 13-specific primers (226, 278, 244, and 238; Table I) that would amplify products of ~300–500 bp if cleavage and polyadenylation had occurred at the downstream signal proximal to the binding site of the upper-strand primer (Fig. 3). pFIN13-specific 3′-RACE PCR products were subcloned and sequenced, revealing that three of the consensus putative cleavage-polyadenylation signals in Flt-1 intron 13 apparently were utilized in HEK293 transfectants: the tandem #1/2 signal and signals #3 and #5 (Fig. 3). Polyadenylation occurred 21 bases downstream of signals #1/2, 13 bases downstream of signal #3, and 80 bases downstream of signal #5 (or 80 bases upstream of signal #6). This site of polyadenylation is unusually far downstream of signal #5 [i.e., greater than 45 bases; Beaudoing et al., 2000]. However, a nested set of non-canonical signals [Beaudoing et al., 2000] lies 32 bases 5′ to the cleavage site and is flanked by upstream and downstream cleavage-promoting elements as described [Reed and Palandjian, 1997]. The potential involvement of these signals in "long" sFlt-1 mRNA processing is addressed experimentally below. To confirm that native mouse sFlt-1 mRNAs also contain a species cleaved and polyadenylated downstream of signal #5, we performed nested 3′-RACE on cDNA derived from mouse lung. This experiment revealed identical cleavage-polyadenylation downstream of signal #5 in both mouse lung and pFIN13 transfectants (Fig. 3). No band corresponding to a product derived from transcripts polyadenylated downstream of signal #4 was observed in either mouse lung or pFIN13 transfectants, even after nested re-amplification.

The transient transfection assay provides a means to determine which cleavage-polyadenylation signals active in Flt-1 intron 13 are important for sFlt-1 protein expression. To confirm the ability of our cDNA and minigene constructs to drive sFlt-1 protein expression, HEK293 cells were transiently transfected with either psFlt-1 or pFIN13, and heparin-adsorbed conditioned media were examined by immunoblotting for the presence of immunoreactive sFlt-1 protein. Media conditioned by psFlt-1 or pFIN13, but not pFlt-1, transfectants contained an anti-Flt-1 (N-terminus) immunoreactive species of M_r 100,000–110,000 (see Fig. 5), consistent with the size of glycosylated sFlt-1 [Kendall et al., 1996]. Lysates of cells transiently or stably transfected with pFlt-1, but not the null vector or psFlt-1, contained a M_r 180,000–200,000 protein strongly reactive with anti-Flt-1 C-terminal antibody (not shown), consistent with the expected size of full-length glycosylated Flt-1 [Waltenberger et al., 1994]. Next, a series of pFIN13 mutants was prepared in which one or more cleavage-polyadenylation signals were deleted [Fig. 4]. None of these deletions altered the putative splice recognition sites or the previously identified mRNA 3′-end [He et al., 1999]. Deletion of all six signals decreased the abundance of sFlt-1 protein in transfectant-conditioned media to scarcely detectable levels (Fig. 5), while deletion of any or all of signals #1–4 did not markedly alter expression, suggesting that remaining signals could fully support pre-RNA processing to a mature, translatable mRNA. In contrast, deletion of signals #5–6 reduced sFlt-1 protein expression by 77%, suggesting that signals #5 and/or #6 may be utilized preferentially, although not exclusively, in the transfected HEK293 cell context. Further deletion of tandem signals #1/2 brought no additional decrease in protein accumulation, whereas deletion of signals #5–6 plus #3 reduced expression to undetectable levels (i.e.,

Fig. 3. (*Overleaf*) 3′-RACE analysis. **A**: Binding sites of primers used to amplify 3′-RACE cDNAs are indicated by arrows (primers and flanking exons not drawn to scale). Locations of sequenced, amplified fragments derived from pFIN13 transfectants (striped bars) or mouse lung cDNA (stippled bar) and their sites of cleavage-polyadenylation relative to consensus signals #1–6 or the site (''5′pA'') previously identified [He et al., 1999] are shown. **B**: Sequences determined by 3′-RACE (lowercase) surrounding observed cleavage-polyadenylation sites (arrows) are shown aligned with intron 13 genomic sequence (uppercase). AP primer reverse-complement, solid underline; consensus cleavage-polyadenylation signals, solid boxes; non-canonical signals, dashed box; putative Upstream Sequence Element, double underline; putative Downstream Sequence Elements, dashed underline. Nucleotide numbering corresponds to that in GenBank accession number AF473823.

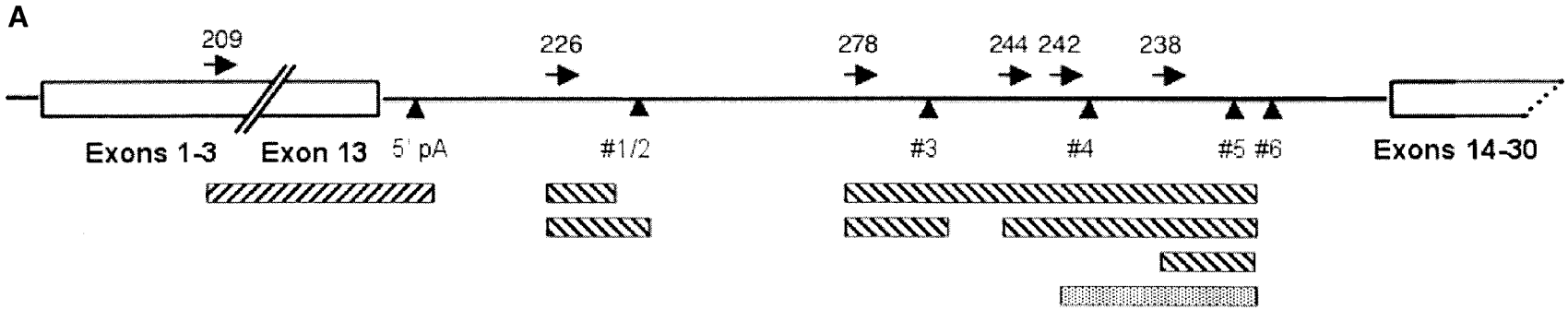

B

...HisValLysHis**End**

5′ Poly A: 213 ...CATGTCAAACATTAAAGGACTCATTTGAAAAGTAACAGTTGTCTCTTATCATCTCAGTTTATTGTTACTGTTGCTAACTTTCA

209/AUAP: ...catgtcaaacattaaaggactcatttgaaaagtaaaaaaaaaaaaaaaaaagtctagtcgacgcgtggcc

---

Internal PolyA: 1280 ...CAAAAGCTAAGAAATTACAAAAAAAAAAAAAGAACAGCATTAAAACTATTTAAGTGCATGCCTTTTTAAATAAAAATAAA...

226/AUAP low: ...caaaagctaagaaattacaaaaaaaaaaaaaaaaagtactagtcgacgcgtggcc

---

PolyA Signal #1,2: 1348 ...AATAAAAATAAATCAAGAGCAATTACACTTTGAACTTGCATTTGAAGGAAAGGTACTTTTAATATGCATTGTTTTTTCTG...

226/AUAP high ...aataaaaataaatcaagagcaattacactttggaaaaaaaaaaaaaaaaaaaaaaaaaaaaaaagtactagtcgacgcgtggcc

---

PolyA Signal #3: 2715 ...AATAAATCCTAATACTGTATGCTTTAGAGGGTGTGTGTGTGTGTGTGTGTGTGTGTGTGTGAACCTTGTTTTTAAATC...

278/AUAP low: ...aataaatcctaatactgtaaaaaaaaaaaaaaaaaaaaaaaaaaaaaaaaaaaaaagtactagtcgacgcgtggcc

---

PolyA Signal #5,6: 4120 ...AATAAATTGTATTGTACCATATTTGTATGTTTTAAGAGAAAATAATATAAAATACAATACTTGTGCTATTATATAGCGCA

278/AUAP high: ...aataaattgtattgtaccatatttgtatgttttaagagaaaataatataaaatacaatacttgtgctattatatagcgca

PolyA Signal #5,6: 4200 AAACCTACAAATTTGTGCCTCTGCCTCTTGAATGAACTTTTTCGTTGCTTGTATTTGGGGGAGAGGGAGGGGAGGGAGGG

278/AUAP high: aaacctaaaaaaaaaaaaaaaaaaaaagtactagtcgacgcgtggcc

PolyA Signal #5,6: 4280 GAGTGACCAATAAAGCATTGAATGATTTCAGAATTTTCCTGTTTGGTCTGCTGCCTCGAAGTGTAGACTATGGAGTAACA...

Fig. 3.

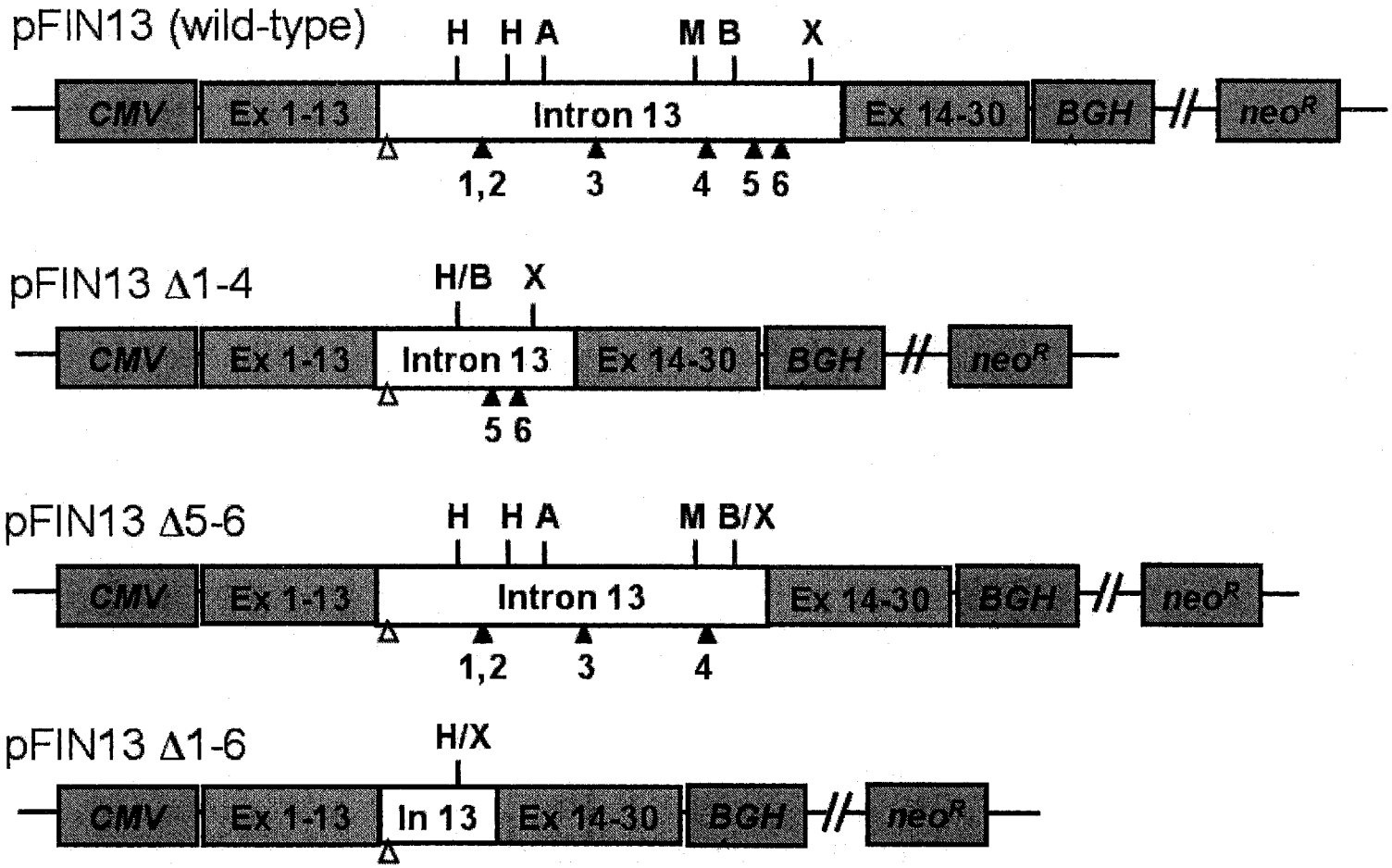

Fig. 4. Flt-1 expression constructs. Structures of the wild-type minigene pFIN13 and deletion mutants are indicated. CMV, human CMV promoter/intron A; BGH, bovine growth hormone polyadenylation signal; neo^R, SV40 promoter and neo^R coding sequence. Sites of the 5′-polyadenylation site [He et al., 1999] (open triangle) and signals #1–6 (filled triangles) are shown (not to scale).

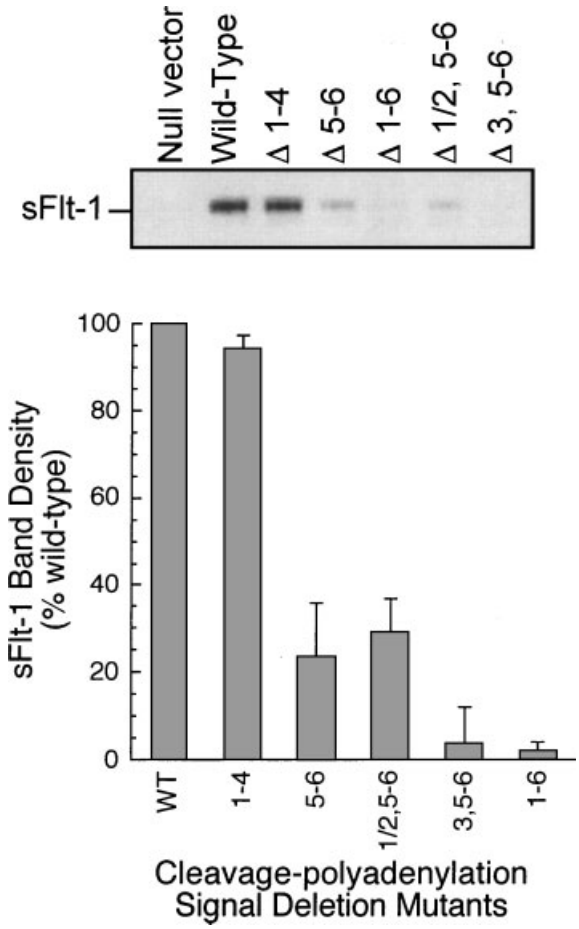

Fig. 5. sFlt-1 expression from minigene constructs. sFlt-1 in heparin-adsorbed conditioned media from HEK293 cells transiently transfected with null vector, wild-type pFIN13, or deletion mutants was detected by immunoblotting with anti-Flt-1 N-terminus antibodies. sFlt-1 band grayscale densities were corrected for background (null-vector) and expressed as a percentage of the corrected wild-type signal. Results shown are mean ± SE from three to seven independent experiments.

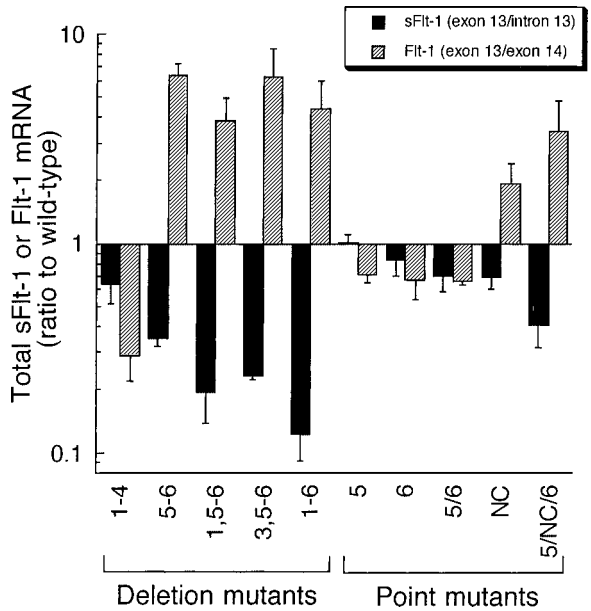

Fig. 6. sFlt-1 and Flt-1 mRNA expression from pFIN13 mutants. Levels of sFlt-1 and Flt-1 mRNA, normalized internally to neo^R mRNA, were determined by QPCR as described in Materials and Methods. All ratios were different from wild-type controls ($P < 0.05$, n = 3–4 independent experiments) except for sFlt-1 expression in the signal #5 or #6 point mutant transfectants. NC, non-canonical cleavage-polyadenylation signal.

similar to the Δ1–6 deletion). Thus, multiple cleavage-polyadenylation signals appear capable of supporting sFlt-1 protein expression.

To evaluate the potential for interaction between RNA processing pathways leading to sFlt-1 and full-length Flt-1, we employed QPCR to measure the relevant mRNAs in HEK293 transfectants. Deletions of cleavage-polyadenylation signals #1–4, #5–6, and #1–6 were associated with progressively larger decreases in normalized sFlt-1 mRNA levels, to 64, 35, and 12% of the wild-type values, respectively (Fig. 6), suggesting that sites contained within the deleted regions are important for sFlt-1 mRNA formation or persistence. Mutants that combined deletion of either signal #1/2 or #3 with deletion of signals #5–6 produced sFlt-1 mRNA levels intermediate between those from the #1–4 and #1–6 deletions. We interpret the measurements of steady-state mRNA levels to reflect rates of formation, although we have not tested the effects of internal deletions on mRNA degradation rates. We suspect that the residual sFlt-1 expression detected by QPCR in the Δ1–6 mutant is attributable to mRNAs that terminate at the site described by He et al. [1999]; this supposition was supported by results of Northern hybridization (not shown).

Interestingly, the decreases in normalized sFlt-1 mRNA levels associated with selected deletions of cleavage-polyadenylation signals were accompanied by reciprocal increases (up to 6.3-fold compared to wild type) in full-length Flt-1 mRNA levels. Since nascent Flt-1 pre-mRNA can be processed to either sFlt-1 or Flt-1 mRNA, this result suggests that the absence of preferred sFlt-1-producing cleavage-polyadenylation signals may allow a given transcript instead to be spliced to form Flt-1 mRNA. An exception to this pattern was seen with the Δ1–4 mutant, which showed reduction in both sFlt-1 and Flt-1 mRNAs. We speculate that a splice

enhancer may reside in the region deleted from this construct.

Results of the deletion mutant studies indicated that the region surrounding cleavage-polyadenylation signals #5 and 6 may be particularly important for sFlt-1 expression in minigene transfectants. To more closely map the RNA sites needed to accomplish cleavage-polyadenylation downstream of signal #5, we prepared a series of point mutations of signals #5, #6 and the intervening non-canonical signals (Fig. 3). These mutations changed signals #5 and #6 to CAGACA and GACAGA, respectively, and the non-canonical signal to CAGACACAGUGCC and were expected to severely reduce cleavage-polyadenylation signaling activity [Sheets et al., 1990]. Mutation of signal #5 or #6 alone had only modest effects on normalized sFlt-1 mRNA levels (no change or 17% decrease relative to wild type, respectively), while the dual signal #5/#6 mutation reduced expression by ~30% (Fig. 6). Surprisingly, with these constructs, Flt-1 mRNA expression also was reduced by 29–35%. Mutation of the non-canonical signal alone produced a 31% decrease in sFlt-1 mRNA levels and a reciprocating increase (1.9-fold) in Flt-1 mRNA. Finally, the combined signal #5/non-canonical/#6 mutant yielded a pattern strongly resembling that seen with the Δ5–6 deletion mutant, with a 60% decrease in sFlt-1 mRNA and 3.4-fold increase in Flt-1 mRNA.

DISCUSSION

The biological effects of VEGF are mediated chiefly by the endothelial cell-surface receptors KDR and Flt-1 [Gerber and Ferrara, 2003]. Alternative pre-mRNA processing leads to the expression of a secreted Flt-1 form, sFlt-1, that retains full VEGF binding potency [Kendall and Thomas, 1993] and, when provided pharmacologically, can inhibit activities of VEGF [Goldman et al., 1998; Kong et al., 1998; Siemeister et al., 1999; Shiose et al., 2000; Takayama et al., 2000]. In view of the dramatic effects of exogenous sFlt-1 on VEGF signaling in vivo, we are interested in defining the molecular mechanisms that govern the pre-mRNA processing events leading to native sFlt-1 expression. Transfection of a Flt-1 minigene construct into HEK293 cells resulted in expression of both secreted (i.e., cleaved-polyadenylated) and transmembrane (spliced) forms of Flt-1 mRNA and protein, indicating that the assay system contained requisite pre-mRNA processing factors. Analysis of 3′-mRNA ends showed that at least four cleavage-polyadenylation signals located in intron 13 were utilized in minigene transfectants (one previously reported [He et al., 1999] plus three novel sites identified in the present work), predicting that multiple distinct native mRNAs for sFlt-1 may be produced. Finally, QPCR analysis of cDNAs derived from cells transfected with deletion- or point-mutants of pFIN13 indicated that cleavage-polyadenylation occurring downstream of putative signal #5 is utilized in preference to the other active signals. This finding was corroborated by Northern RNA hybridization analysis, using an intron 13-selective probe, of total RNA recovered from pFIN13-transfected cells, which revealed a predominant species at the size (6.3 kb) predicted for transcripts processed downstream of signal #5.

These findings have implications for the interpretation of previous Flt-1 expression results. For example, an active cleavage-polyadenylation signal near the 3′-end of intron 13 would produce a native sFlt-1 mRNA ~6.5–7.0 kb in length. Therefore, the 6.5–8.5 kb family of bands identified as full-length Flt-1 on Northern blots by numerous other investigators [Shibuya et al., 1990; Yamane et al., 1994; Li et al., 1996; Detmar et al., 1997; Graubert et al., 2001] may in fact include an sFlt-1 mRNA species. He et al. [1999], using a probe specific for the extreme 5′-end of intron 13, found that mouse placenta contains a predominant sFlt-1 mRNA of ~3 kb, consistent with cleavage-polyadenylation at the site identified by their 3′-RACE analysis. However, their published blots also reveal a larger, minor sFlt-1-hybridizing species that co-migrates with the major band identified using a full-length Flt-1-specific probe. More detailed analysis is required to determine the relative abundance and biochemical properties of the various sFlt-1-encoding mRNA species in native tissues.

A limitation of our studies is that our 8-kb Flt-1 minigene construct cannot reflect the influence of other flanking introns or the native separation of adjacent exons. In addition, we acknowledge that use of a non-endothelial transfection host may not faithfully reproduce all aspects of sFlt-1 expression control. Nevertheless, it is significant that cDNAs derived from numerous mouse tissues likewise showed

evidence of an sFlt-1 mRNA polyadenylated downstream of signal #5 (Figs. 2 and 3), indicating that usage of this site is not confined to our experimental model. Moreover, a search of the NCBI mouse EST databases revealed six independent entries that reflect polyadenylation at this site. Finally, the finding of a potential mechanism for selective changes in Flt-1 and sFlt-1 expression is consistent with reports of altered ratios of the two species physiologically [Clark et al., 1998; He et al., 1999; Krussel et al., 1999].

Taken together, our results indicate that a fraction of native sFlt-1 mRNAs is cleaved and polyadenylated near the 3′-end of intron 13, resulting in a UTR of ~4,060 bases in length. The Flt-1-hybridizing mRNA species of 2.2–3.0 kb reported by other investigators [Shibuya et al., 1990; Yamane et al., 1994] likely represent sFlt-1 mRNA isoforms polyadenylated at 5′-sites previously reported [He et al., 1999; Mezquita et al., 2003] or the novel sites #1/2 and #3 reported here. Overall, these mRNAs would differ in length by as much as 3.9 kb in their 3′-UTRs, a site of potential regulatory importance [Conne et al., 2000]. Thus, an opportunity may exist for cells to regulate sFlt-1 protein expression, at a constant rate of Flt-1 gene transcription, by the selective use of cleavage-polyadenylation sites and consequent production of mRNAs differing in stability, intracellular targeting, and translation efficiency.

Two of the three active cleavage-polyadenylation sites newly identified for sFlt-1 mRNA formation in the current studies adhere closely to the consensus pattern described by other investigators. Specifically, cleavage occurs within an interval 11–23 bases downstream of the AAUAAA motifs #1/2 and #3 [Chen et al., 1995], and in both cases the cleavage sites are followed within 6–25 bases by U-rich or GU-rich tracts [Chou et al., 1994; Graber et al., 1999]. Signal #5, however, is an exception, since cleavage occurs unusually far downstream (80 bases) from the AAUAAA tract (or 80 bases upstream of signal #6). It is possible that this site is signaled by AAUAAA #5 (or #6) but processed in an unusual fashion owing to unrecognized structural features. Alternatively, we considered that the nested non-canonical sequences [AAUAUA, UAUAAA, or AAUACA; Chou et al., 1994] that lie 32 bases upstream of the cleavage site participate in signaling of cleavage-polyadenylation. Results of point mutation experiments (Fig. 6) suggest that no individual hexameric locus is exclusively responsible for the bulk of the signaling; only combined mutation of signals #5, #6 and the intervening non-canonical tract could reduce sFlt-1 mRNA to levels approaching that seen with outright deletion of the region. We speculate that full signaling function may require cooperativity among all three sites, or that any of the three signals, if intact, can largely suffice. We are currently characterizing the binding of RNA processing factors to these regions in cell-free preparations. The importance of the 3′-end of Flt-1 intron 13 also is suggested by the extraordinary similarity (85.6% identity within a 396-bp region encompassing cleavage-polyadenylation signals #5 and 6) between our mouse sequence and that of human Flt-1 intron 13 (GenBank NT_024525). This homology far exceeds that observed in the rest of the non-sFlt-1-coding portions of intron 13 and may reflect the presence of conserved functional domains in transcripts from the two species.

In our studies, decreases in sFlt-1 mRNA associated with cleavage-polyadenylation signal mutations were, in most cases, accompanied by reciprocal increases in Flt-1 mRNA levels. This result suggests that the absence of preferred sFlt-1-producing cleavage-polyadenylation signaling elements may allow a given transcript instead to be spliced to form Flt-1 mRNA. We postulate that regulatory mechanisms may exist to control the balance between intron splicing (to form full-length Flt-1) and cleavage-polyadenylation (to produce sFlt-1). A strong parallel is found in the formation of mRNAs encoding secreted IgM during B lymphocyte maturation, which may be described as a regulated competition between splicing and cleavage-polyadenylation signals residing in the same intron [Peterson, 1992]. As with IgM expression, changes in the abundance or activities of RNA processing factors [Takagaki et al., 1996] may be crucial to establishing the distribution between Flt-1 and sFlt-1 mRNAs. In turn, this balance may be an important determinant of endothelial responsiveness to VEGF. Other studies in our laboratory have revealed that loss of intron 13 splicing efficiency in 3′-polypyrimidine tract mutants is coupled to an increase in sFlt-1 mRNA expression (Roche RI and Huckle WR, unpublished data). These 3′-splicing elements lie only 550 bases downstream of cleavage-polyadenylation signal #6,

suggesting that RNA-binding factors responsible for spliceosome assembly, (e.g., U2 snRNP) [Reed and Palandjian, 1997] and cleavage-polyadenylation (CstF and CPSF) [Zhao et al., 1999] may be drawn into close proximity, presenting an opportunity for consequential interference between the two processes.

We believe that elucidation of post-transcriptional mechanisms controlling sFlt-1 expression will clarify the role that this endogenous inhibitor of VEGF plays in adaptive cardiac angiogenesis, peripheral vascular disease, tumor vascularization, and diabetic retinopathy. Although the human and rodent genome sequencing projects have generated a wealth of information on the primary structure of introns, our ability to recognize sites of regulatory significance a priori is limited. Understanding the novel features of sFlt-1 expression thus may provide more comprehensive insights into pre-mRNA processing.

ACKNOWLEDGMENTS

The authors thank Dan Ward for guidance with statistical analysis.

REFERENCES

Barleon B, Totzke F, Herzog C, Blanke S, Kremmer E, Siemeister G, Marme D, Martiny-Baron G. 1997. Mapping of the sites for ligand binding and receptor dimerization at the extracellular domain of the vascular endothelial growth factor receptor FLT-1. J Biol Chem 272:10382–10388.

Beaudoing E, Freier S, Wyatt JR, Claverie JM, Gautheret D. 2000. Patterns of variant polyadenylation signal usage in human genes. Genome Res 10:1001–1010.

Carmeliet P. 2003. Angiogenesis in health and disease. Nat Med 9:653–660.

Celletti FL, Hilfiker PR, Ghafouri P, Dake MD. 2001. Effect of human recombinant vascular endothelial growth factor-165 on progression of atherosclerotic plaque. J Am Coll Cardiol 37:2126–2130.

Chen F, MacDonald CC, Wilusz J. 1995. Cleavage site determinants in the mammalian polyadenylation signal. Nucleic Acids Res 23:2614–2620.

Choi K, Wall C, Hanratty R, Keller G. 1994. Isolation of a gene encoding a novel receptor tyrosine kinase from differentiated embryonic stem cells. Oncogene 9:1261–1266.

Chou ZF, Chen F, Wilusz J. 1994. Sequence and position requirements for uridylate-rich downstream elements of polyadenylation signals. Nucleic Acids Res 22:2525–25231.

Clark DE, Smith SK, He Y, Day KA, Licence DR, Corps AN, Lammoglia R, Charnock-Jones DS. 1998. A vascular endothelial growth factor antagonist is produced by the human placenta and released into the maternal circulation. Biol Reprod 59:1540–1548.

Conne B, Stutz A, Vassalli JD. 2000. The 3′ untranslated region of messenger RNA: A molecular 'hotspot' for pathology? Nat Med 6:637–641.

Detmar M, Brown LF, Berse B, Jackman RW, Elicker BM, Dvorak HF, Claffey KP. 1997. Hypoxia regulates the expression of vascular permeability factor/vascular endothelial growth factor (VPF/VEGF) and its receptors in human skin. J Invest Dermatol 108:263–268.

Epstein SE, Fuchs S, Zhou YF, Baffour R, Kornowski R. 2001. Therapeutic interventions for enhancing collateral development by administration of growth factors: Basic principles, early results and potential hazards. Cardiovasc Res 49:532–542.

Finnerty H, Kelleher K, Morris GE, Bean K, Merberg DM, Kriz R, Morris JC, Sookdeo H, Turner KJ, Wood CR. 1993. Molecular cloning of murine FLT and FLT4. Oncogene 8:2293–2298.

Folkman J. 2001. Angiogenesis-dependent diseases. Semin Oncol 28:536–542.

Frohman MA, Dush MK, Martin GR. 1988. Rapid production of full-length cDNAs from rare transcripts: Amplification using a single gene-specific oligonucleotide primer. Proc Natl Acad Sci USA 85:8998–9002.

Gerber HP, Ferrara N. 2003. The role of VEGF in normal and neoplastic hematopoiesis. J Mol Med 81:20–31.

Goldman CK, Kendall RL, Cabrera G, Soroceanu L, Heike Y, Gillespie GY, Siegal GP, Mao X, Bett AJ, Huckle WR, Thomas KA, Curiel DT. 1998. Paracrine expression of a native soluble vascular endothelial growth factor receptor inhibits tumor growth, metastasis, and mortality rate. Proc Natl Acad Sci USA 95:8795–8800.

Graber JH, Cantor CR, Mohr SC, Smith TF. 1999. In silico detection of control signals: mRNA 3′-end-processing sequences in diverse species. Proc Natl Acad Sci USA 96:14055–14060.

Graubert MD, Ortega MA, Kessel B, Mortola JF, Iruela-Arispe ML. 2001. Vascular repair after menstruation involves regulation of vascular endothelial growth factor-receptor phosphorylation by sFLT-1. Am J Pathol 158: 1399–1410.

He Y, Smith SK, Day KA, Clark DE, Licence DR, Charnock-Jones DS. 1999. Alternative splicing of vascular endothelial growth factor (VEGF)-R1 (FLT-1) pre-mRNA is important for the regulation of VEGF activity. Mol Endocrinol 13:537–545.

Huckle WR, Roche RI. 2001. Regulation of expression of sFlt-1, an endogenous inhibitor of VEGF-stimulated angiogenesis. Mol Biol Cell 12(Suppl):229a–230a.

Ishii TM, Zerr P, Xia XM, Bond CT, Maylie J, Adelman JP. 1998. Site-directed mutagenesis. Methods Enzymol 293: 53–71.

Kendall RL, Thomas KA. 1993. Inhibition of vascular endothelial cell growth factor activity by an endogenously encoded soluble receptor. Proc Natl Acad Sci USA 90:10705–10709.

Kendall RL, Wang G, Thomas KA. 1996. Identification of a natural soluble form of the vascular endothelial growth factor receptor, FLT-1, and its heterodimerization with KDR. Biochem Biophys Res Commun 226:324–328.

Kim KJ, Li B, Winer J, Armanini M, Gillett N, Phillips HS, Ferrara N. 1993. Inhibition of vascular endothelial growth factor-induced angiogenesis suppresses tumour growth in vivo. Nature 362:841–844.

Kondo K, Hiratsuka S, Subbalakshmi E, Matsushime H, Shibuya M. 1998. Genomic organization of the flt-1 gene encoding for vascular endothelial growth factor (VEGF) receptor-1 suggests an intimate evolutionary relationship between the 7-Ig and the 5-Ig tyrosine kinase receptors. Gene 208:297–305.

Kong HL, Hecht D, Song W, Kovesdi I, Hackett NR, Yayon A, Crystal RG. 1998. Regional suppression of tumor growth by in vivo transfer of a cDNA encoding a secreted form of the extracellular domain of the flt-1 vascular endothelial growth factor receptor. Hum Gene Ther 9: 823–833.

Krussel JS, Casan EM, Raga F, Hirchenhain J, Wen Y, Huang HY, Bielfeld P, Polan ML. 1999. Expression of mRNA for vascular endothelial growth factor transmembraneous receptors Flt1 and KDR, and the soluble receptor sflt in cycling human endometrium. Mol Hum Reprod 5:452–458.

Li J, Brown LF, Hibberd MG, Grossman JD, Morgan JP, Simons M. 1996. VEGF, flk-1, and flt-1 expression in a rat myocardial infarction model of angiogenesis. Am J Physiol 270:H1803–H1811.

Livak KJ, Schmittgen TD. 2001. Analysis of relative gene expression data using real-time quantitative PCR and the $2^{-\text{Delta Delta C(T)}}$ method. Methods 25:402–408.

Livak KJ, Flood SJ, Marmaro J, Giusti W, Deetz K. 1995. Oligonucleotides with fluorescent dyes at opposite ends provide a quenched probe system useful for detecting PCR product and nucleic acid hybridization. PCR Methods Appl 4:357–362.

Los M, Voest EE. 2001. The potential role of antivascular therapy in the adjuvant and neoadjuvant treatment of cancer. Semin Oncol 28:93–105.

Mezquita J, Mezquita B, Pau M, Mezquita C. 2003. Down-regulation of Flt-1 gene expression by the proteasome inhibitor MG262. J Cell Biochem 89:1138–1147.

Nguyen LL, D'Amore PA. 2001. Cellular interactions in vascular growth and differentiation. Int Rev Cytol 204: 1–48.

Osoegawa K, Tateno M, Woon PY, Frengen E, Mammoser AG, Catanese JJ, Hayashizaki Y, deJong PJ. 2000. Bacterial artificial chromosome libraries for mouse sequencing and functional analysis. Genome Res 10:116–128.

Pavco PA, Bouhana KS, Gallegos AM, Agrawal A, Blanchard KS, Grimm SL, Jensen KL, Andrews LE, Wincott FE, Pitot PA, Tressler RJ, Cushman C, Reynolds MA, Parry TJ. 2000. Antitumor and antimetastatic activity of ribozymes targeting the messenger RNA of vascular endothelial growth factor receptors. Clin Cancer Res 6:2094–2103.

Peterson ML. 1992. Balanced efficiencies of splicing and cleavage-polyadenylation are required for mu-s and mu-m mRNA regulation. Gene Expr 2:319–327.

Prewett M, Huber J, Li Y, Santiago A, O'Connor W, King K, Overholser J, Hooper A, Pytowski B, Witte L, Bohlen P, Hicklin DJ. 1999. Antivascular endothelial growth factor receptor (fetal liver kinase 1) monoclonal antibody inhibits tumor angiogenesis and growth of several mouse and human tumors. Cancer Res 59:5209–5218.

Reed R, Palandjian L. 1997. Spliceosome assembly. In: Krainer AR, editor. Eukaryotic mRNA processing. Oxford: IRL Press. pp 103–129.

Shawver LK, Lipson KE, Fong TAT, McMahon G, Plowman GD, Strawn LM. 1997. Receptor tyrosine kinases as targets for inhibition of angiogenesis. Drug Dev Today 2:50–63.

Sheets MD, Ogg SC, Wickens MP. 1990. Point mutations in AAUAAA and the poly (A) addition site: Effects on the accuracy and efficiency of cleavage and polyadenylation in vitro. Nucleic Acids Res 18:5799–5805.

Shibuya M, Yamaguchi S, Yamane A, Ikeda T, Tojo A, Matsushime H, Sato M. 1990. Nucleotide sequence and expression of a novel human receptor-type tyrosine kinase gene (flt) closely related to the fms family. Oncogene 5:519–524.

Shiose S, Sakamoto T, Yoshikawa H, Hata Y, Kawano Y, Ishibashi T, Inomata H, Takayama K, Ueno H. 2000. Gene transfer of a soluble receptor of VEGF inhibits the growth of experimental eyelid malignant melanoma. Invest Ophthalmol Vis Sci 41:2395–2403.

Siemeister G, Schirner M, Weindel K, Reusch P, Menrad A, Marme D, Martiny-Baron G. 1999. Two independent mechanisms essential for tumor angiogenesis: Inhibition of human melanoma xenograft growth by interfering with either the vascular endothelial growth factor receptor pathway or the Tie-2 pathway. Cancer Res 59: 3185–3191.

Spranger J, Pfeiffer AF. 2001. New concepts in pathogenesis and treatment of diabetic retinopathy. Exp Clin Endocrinol Diabetes 109:S438–S450.

Takagaki Y, Seipelt RL, Peterson ML, Manley JL. 1996. The polyadenylation factor CstF-64 regulates alternative processing of IgM heavy chain pre-mRNA during B cell differentiation. Cell 87:941–952.

Takayama K, Ueno H, Nakanishi Y, Sakamoto T, Inoue K, Shimizu K, Oohashi H, Hara N. 2000. Suppression of tumor angiogenesis and growth by gene transfer of a soluble form of vascular endothelial growth factor receptor into a remote organ. Cancer Res 60:2169–2177.

Waltenberger J, Claesson-Welsh L, Siegbahn A, Shibuya M, Heldin CH. 1994. Different signal transduction properties of KDR and Flt1, two receptors for vascular endothelial growth factor. J Biol Chem 269:26988–26995.

Yamane A, Seetharam L, Yamaguchi S, Gotoh N, Takahashi T, Neufeld G, Shibuya M. 1994. A new communication system between hepatocytes and sinusoidal endothelial cells in liver through vascular endothelial growth factor and Flt tyrosine kinase receptor family (Flt-1 and KDR/Flk-1). Oncogene 9:2683–2690.

Yancopoulos GD, Davis S, Gale NW, Rudge JS, Wiegand SJ, Holash J. 2000. Vascular-specific growth factors and blood vessel formation. Nature 407:242–248.

Zhao J, Hyman L, Moore C. 1999. Formation of mRNA 3′ ends in eukaryotes: Mechanism, regulation, and interrelationships with other steps in mRNA synthesis. Microbiol Mol Biol Rev 63:405–445.